SI Appendix

Riboswitches for the alarmone ppGpp expand the collection of RNA-based signaling systems

Madeline E. Sherlock,[1] Narasimhan Sudarsan,[2] Ronald R. Breaker[1,2,3]*

[1]Department of Molecular Biophysics and Biochemistry, [2]Howard Hughes Medical Institute, [3]Department of Molecular, Cellular and Developmental Biology, Yale University, P.O. Box 208103, New Haven, CT 06520-8103, USA.

www.pnas.org/cgi/doi/10.1073/pnas.1720406115

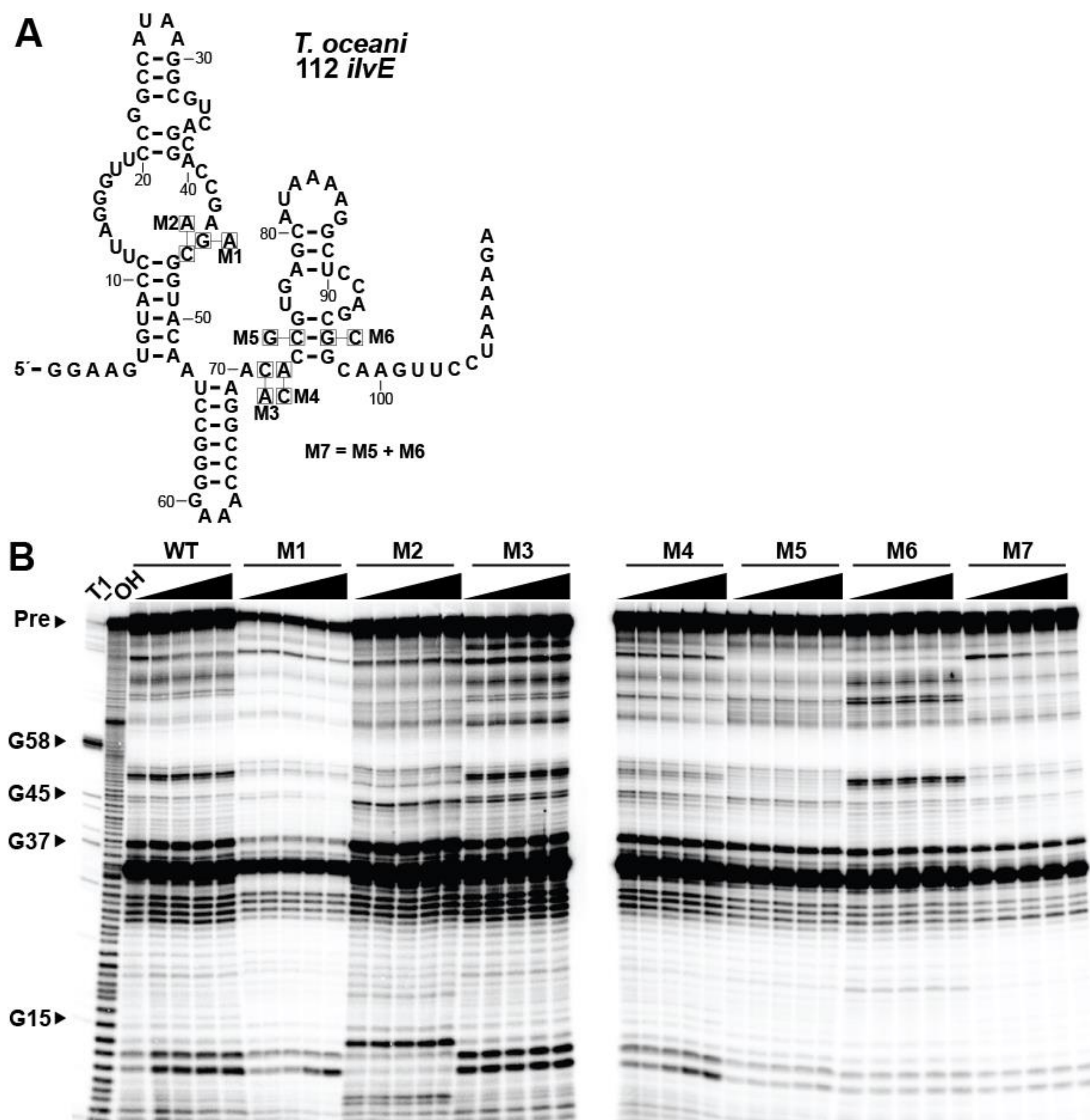

Fig. S1. Mutation of conserved nucleotides disrupt ppGpp binding. (*A*) Sequence and secondary structure of the 112 *ilvE* RNA from *T. oceani*. Single nucleotide positions that were altered to produce each mutant RNA are identified with boxes, annotated with the nucleotide identity of each mutation, and labeled M1 through M6. M7 contains mutations at both positions specified by M5 and M6. (*B*) PAGE analysis of in-line probing assays with WT and mutated sequences of the 112 *ilvE* RNA in the presence of 0, 100 nM, 1 µM, 10 µM, or 100 µM ppGpp. Additional annotations are as described in the legend to **Fig. 2*B***. Note that, for the mutant constructs, either no modulation (M2, M3, M5, M6) or very little modulation (M1, M4) is observed only at the highest ppGpp concentrations tested (10 µM and100 µM). Because the K_D measured for the WT

construct is 10 nM, this means that most mutant constructs experience at least three orders of magnitude loss of affinity.

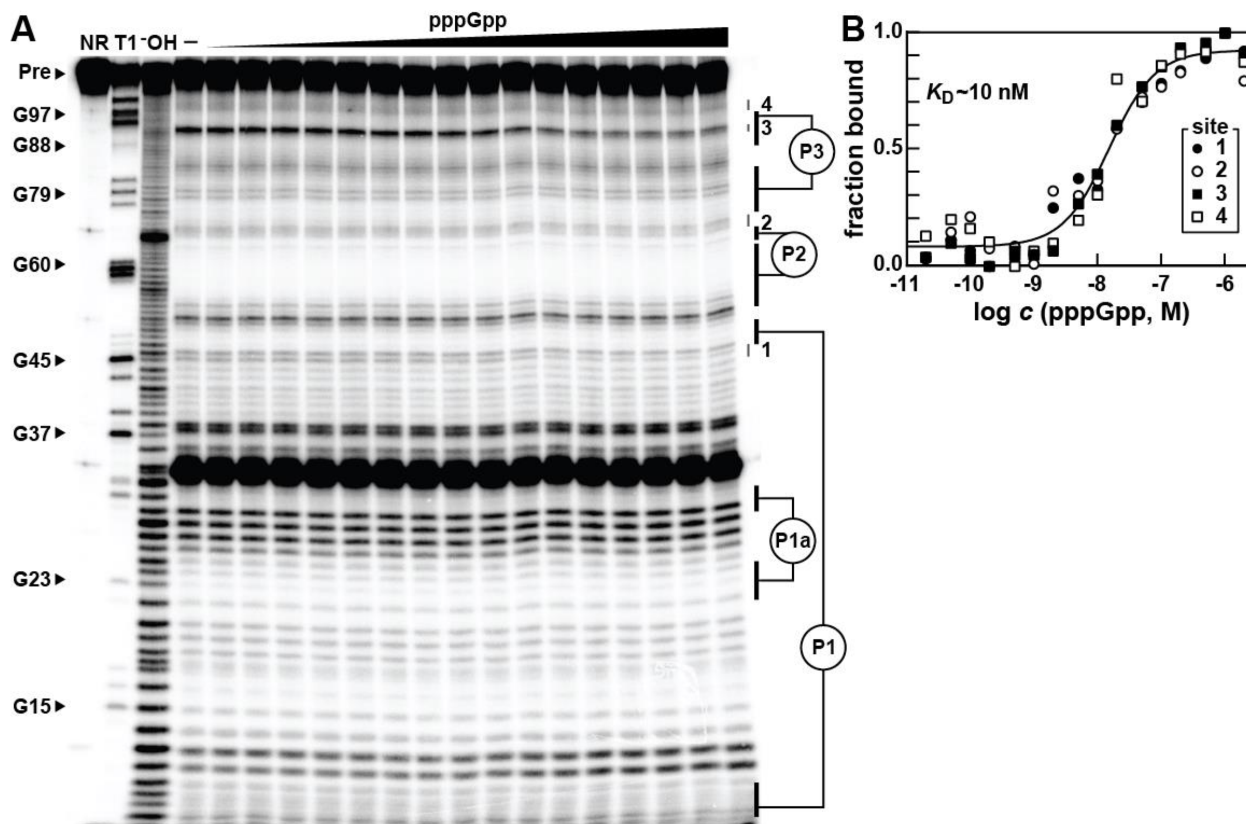

Fig. S2. Recognition of pppGpp by a riboswitch aptamer. (*A*) PAGE analysis of the products of in-line probing of 5′-^{32}P-labeled 112 *ilvE* RNA in the presence of increasing pppGpp concentrations. In-line probing experiments contained either no ligand (–) or pppGpp ranging from 20 pM to 2 μM. Annotations are as described for **Fig. 2*B***. (*B*) Plot of the fraction of RNA bound by pppGpp, as determined by the normalized fraction of RNA scission at regions 1 through 4 as a function of the logarithm of pppGpp concentration. Additional details are as describe in the legend to **Fig. 2*C***.

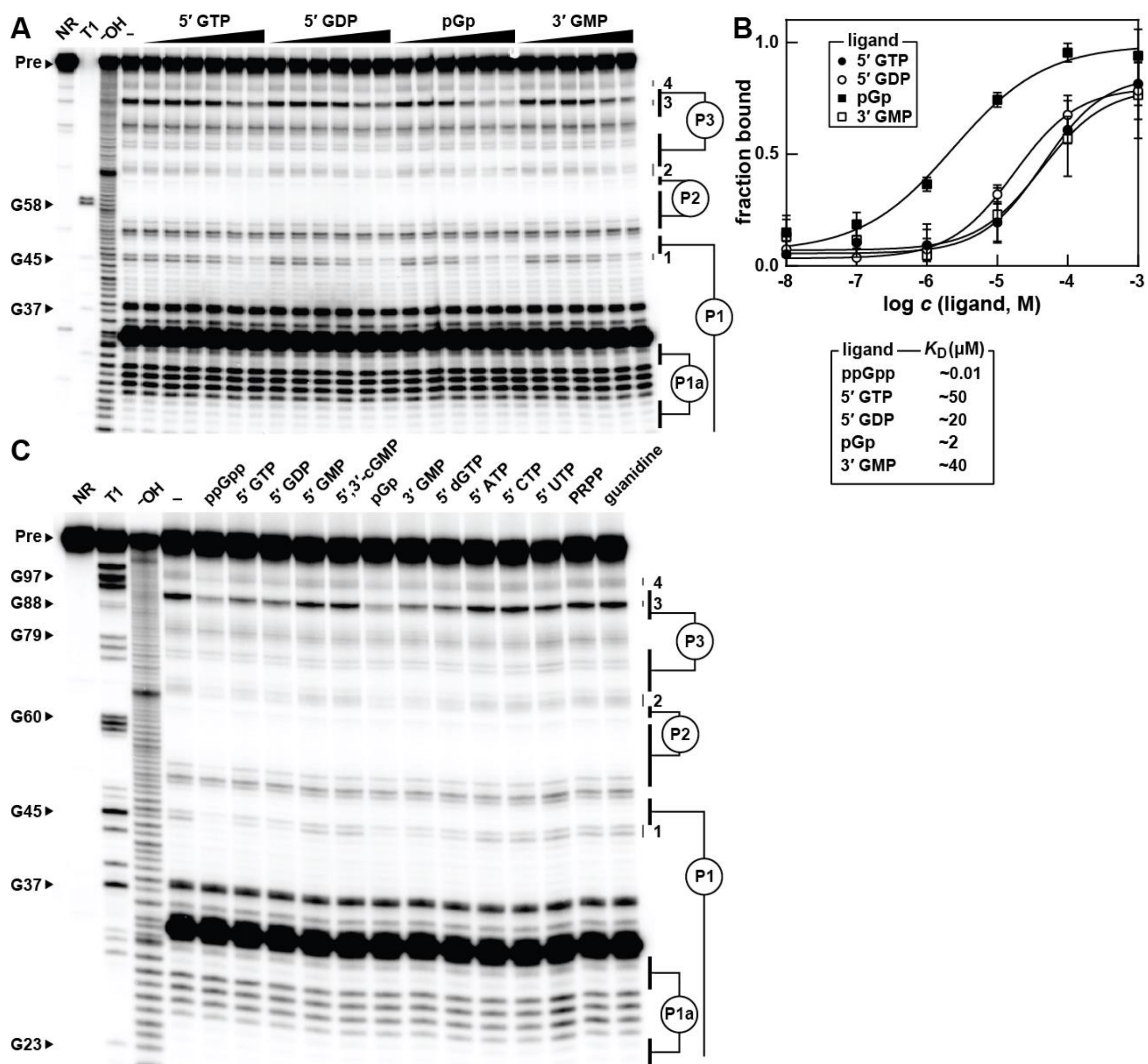

Fig. S3. Binding selectivity of a representative ppGpp riboswitch. (*A*) PAGE analysis of in-line probing reactions of the 112 *ilvE* aptamer from *T. oceani* (see **Fig. 2*A***) in the presence of structural analogs of ppGpp that exhibited structural modulation. Each compound was tested at 10 nM, 100 nM, 1 µM, 10 µM, 100 µM, and 1 mM. Annotations are as described for **Fig. 2*B***. (*B*) Plot of the fraction of RNA bound by each ligand, as determined by the average and standard deviation of the normalized fraction of RNA scission at regions 1-4 as a function of the logarithm of ligand concentration. Additional details are as describe in the legend to **Fig. 2*C***. (*C*) PAGE analysis of in-line probing reactions of the 112 *ilvE* aptamer in the presence of 100 µM concentration of various analogs of ppGpp, nucleotides, or the known ligands of other *ykkC* motif RNA subtypes (PRPP and guanidine).

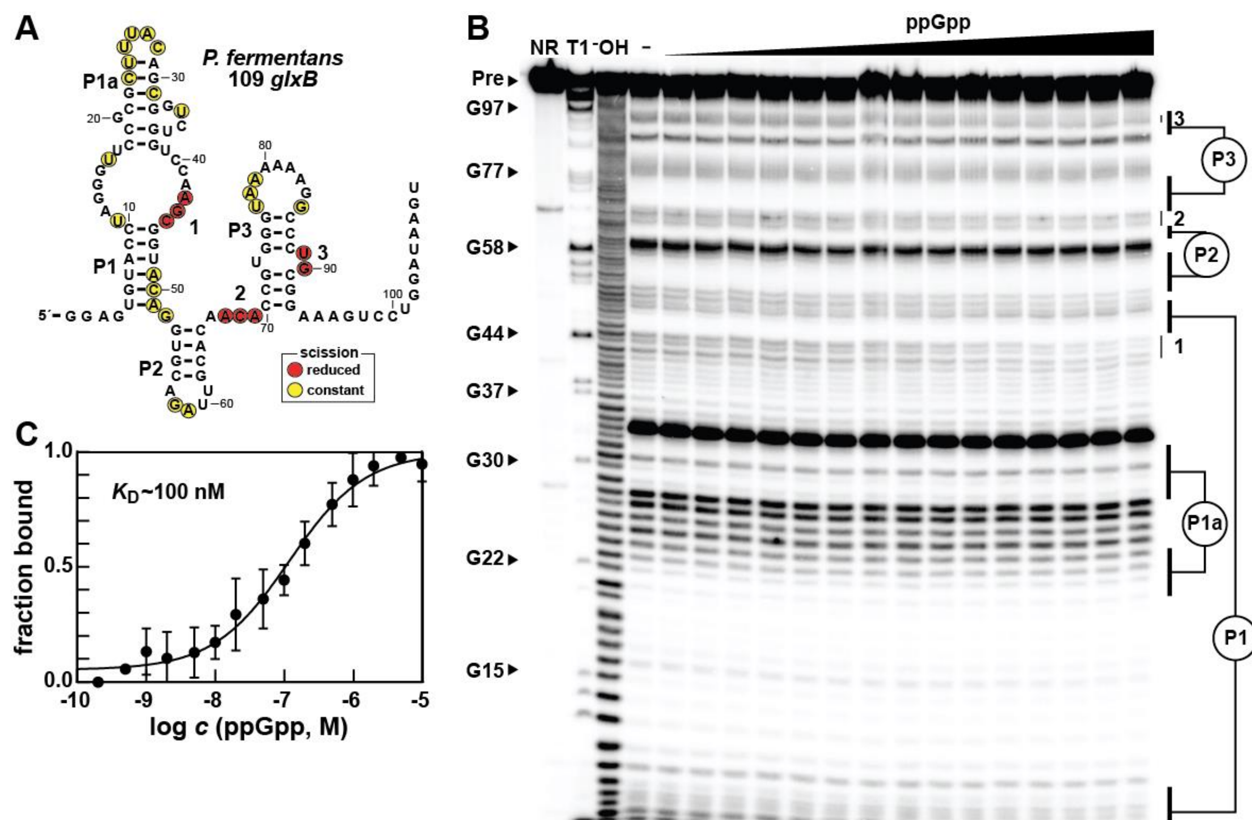

Fig. S4. Ligand binding by an additional ppGpp riboswitch aptamer representative found upstream of glutamate synthase genes. (*A*) Sequence and secondary structure of the 109 nucleotide RNA derived from the *glxB* gene of *Pelosinus fermentans*. Data collected in *B* were used to determine regions of constant or reduced scission upon the addition of ppGpp to in-line probing assays. (*B*) PAGE analysis of the products of in-line probing of 5′-^{32}P-labeled 109 *glxB* RNA in the presence of increasing ppGpp concentrations. Annotations are as described for Figure 2B. In-line probing experiments contained either no ligand (–) or ppGpp ranging from 200 pM to 10 μM. Regions 1-3 of the RNA exhibit structural stabilization in a ppGpp-dependent manner. Note that this banding pattern and the pattern of changes resulting from in-line probing assay reactions are not identical to those observed for the original *T. oceani ilvE* construct presented in **Fig. 2**. The distinct nucleotide sequences of these representatives will exhibit patterns specific to these individual constructs. (*C*) Plot of the fraction of 109 *glxB* RNA bound to ligand as a function of the logarithm of ppGpp concentration. The fraction bound value plotted at each ppGpp concentration is the average of the values derived from band intensities at regions 1, 2 and 3 after normalization to a value between 1 (band intensity in the absence of ppGpp) and 0 (band intensity at maximum ppGpp concentration). The fraction bound value equals 1 minus

the band intensity value. Error bars indicate standard deviation. Additional details are as describe in the legend to **Fig. 2*C***.

Fig. S5. Ligand binding by an additional ppGpp riboswitch aptamer representative found upstream of *natA*. (*A*) Sequence and secondary structure of the 104 nucleotide RNA derived from the *natA* gene of *Clostridium sp. BL8*. Data collected in *B* were used to determine regions of constant or reduced scission upon the addition of ppGpp to in-line probing assays. (*B*) PAGE analysis of the products of in-line probing of 5′-^{32}P-labeled 104 *natA* RNA in the presence of increasing ppGpp concentrations. Annotations are as described for Figure 2B. In-line probing experiments contained either no ligand (–) or ppGpp ranging from 200 pM to 10 µM. Regions 1-3 of the RNA exhibit structural stabilization in a ppGpp-dependent manner. Note that this banding pattern and the pattern of changes resulting from in-line probing assay reactions are not identical to those observed for the original *T. oceani ilvE* construct presented in **Fig. 2**. The distinct nucleotide sequences of these representatives will exhibit patterns specific to these individual constructs. (*C*) Plot of the fraction of 104 *natA* RNA bound to ligand as a function of

the logarithm of ppGpp concentration. The fraction bound value plotted at each ppGpp concentration was derived as described in the legend to **SI Appendix**, **Fig. S4**. Additional details are as describe in the legend to **Fig. 2*C***.

Supplementary Table 1 │ Sequences of synthetic DNAs used in this study.

Name	Sequence	Annotation
MES137	TAATACGACTCACTATAGG AAGTGTACCTTAGGGTTCC GGCCATAAGGCGTCAGCG ACCGAGCGGTACAATCCG GGG	Forward template for transcription of the WT *T. oceani* 112 *ilvE* RNA
MES138	TCTTTTAGGAACTTGCCGC TGGAGCCTTTTATGCTCAC GGTGTTCCGGGTTTCCCCG GATTGTACCGCTCGG	Reverse template for transcription of the WT *T. oceani* 112 *ilvE* RNA
MES177	TAATACGACTCACTATAGG AAGTGTACCTTAGGGTTCC GGCCATAAGGCGTCAGCG ACCGAACGGTACAATCCG GGG	Forward template for transcription of the M1 *T. oceani* 112 *ilvE* RNA
MES178	TCTTTTAGGAACTTGCCGC TGGAGCCTTTTATGCTCAC GGTGTTCCGGGTTTCCCCG GATTGTACCGTTCGG	Reverse template for transcription of the M1 *T. oceani* 112 *ilvE* RNA
MES179	TAATACGACTCACTATAGG AAGTGTACCTTAGGGTTCC GGCCATAAGGCGTCAGCG ACCGAGAGGTACAATCCG GGG	Forward template for transcription of the M2 *T. oceani* 112 *ilvE* RNA
MES180	TCTTTTAGGAACTTGCCGC TGGAGCCTTTTATGCTCAC GGTGTTCCGGGTTTCCCCG GATTGTACCTCTCGG	Reverse template for transcription of the M2 *T. oceani* 112 *ilvE* RNA
MES181	TCTTTTAGGAACTTGCCGC TGGAGCCTTTTATGCTCAC GGTTTTCCGGGTTTCCCCG GATTGTACCGCTCGG	Reverse template for transcription of the M3 *T. oceani* 112 *ilvE* RNA
MES182	TCTTTTAGGAACTTGCCGC TGGAGCCTTTTATGCTCAC GGGGTTCCGGGTTTCCCCG GATTGTACCGCTCGG	Reverse template for transcription of the M4 *T. oceani* 112 *ilvE* RNA
MES183	TCTTTTAGGAACTTGCCGC TGGAGCCTTTTATGCTCAC CGTGTTCCGGGTTTCCCCG GATTGTACCGCTCGG	Reverse template for transcription of the M5 *T. oceani* 112 *ilvE* RNA
MES184	TCTTTTAGGAACTTGCGGC TGGAGCCTTTTATGCTCAC GGTGTTCCGGGTTTCCCCG GATTGTACCGCTCGG	Reverse template for transcription of the M6 *T. oceani* 112 *ilvE* RNA

MES144	TCTTTTAGGAACTTGCGGC TGGAGCCTTTTATGCTCAC CGTGTTCCGGGTTTCCCCG GATTGTACCGCTCGG	Reverse template for transcription of the M7 *T. oceani* 112 *ilvE* RNA
MES207	TCTTTTAGGAACTTGCCGC TGGAGCCTTTTATGCTCAC GGTATTCCGGGTTTCCCCG GATTGTACCGCTCGG	Reverse template for transcription of the M8 *T. oceani* 112 *ilvE* RNA
MES208	TAATACGACTCACTATAGG AGTGTACCTAGGGTTCCGC GCTTTACAGCGGTCTGGTC CAAGCGGTACAGGTGC	Forward template for transcription of the WT *P. fermentans* 109 *glxB* RNA
MES209	ACTTATCCAGGACTTTCCG CAGGGCCTTTTTACCCAC GGTGTTGTGCAATCTGCAC CTGTACCGCTTGGACC	Reverse template for transcription of the WT *P. fermentans* 109 *glxB* RNA
MES212	TAATACGACTCACTATAGG AGAGTGCATCTAGGGTTCC GATGGAAACATGTCTGGTC CGAGCGATGCAGG	Forward template for transcription of the WT *Clostridium sp. BL8* 104 *natA* RNA
MES213	CATAGGTTGAGACTCGTCC TTTAGGCTTTTTTCCTAAA AGTGTAGATAAAATCCTGC ATCGCTCGGACCAGAC	Reverse template for transcription of the WT *Clostridium sp. BL8* 104 *natA* RNA
MES153	GCGCACATGAGAATTCCAG CGACGCTGTTGATCCTTTT AAATAAGTCTGATAAAATG TGAACTAAAGTTATAAATG AAAGAATGTATTATAACAG CAGGAAGTGTACCTAGGGT TCCGGGAGCTGCTCCGTCT GGTCCGAGCGGTACAAAA TCCAGAGCATGGATTTACA CCGTGGGCAGAAAATACC CGAGCGGAAAGTTCCTCGA GAGGGTAGGAACACCGCT CGGTTTTCTATAATATTCA GAGGATCCCCAGCTGCGC	IDT G-block containing the WT *D. hafniense ilvE* riboswitch and controlled by the *B. subtilis lysC* promoter, for serving as a dsDNA template for *in vitro* transcription termination assays
MES154	GCGCACATGAGAATTCCAG CGACGCTGTTGATCCTTTT AAATAAGTCTGATAAAATG TGAACTAAAGTTATAAATG AAAGAATGTATTATAACAG CAGGAAGTGTACCTAGGGT TCCGGGAGCTGCTCCGTCT GGTCCGAGAGGTACAAAA	IDT G-block containing the mutation of a conserved nucleotide (M9) *D. hafniense* riboswitch and controlled by the *B. subtilis lysC* promoter, for serving as a dsDNA template for *in vitro* transcription termination assays

	TCCAGAGCATGGATTTACA CCGTGGGCAGAAAATACC CGAGCGGAAAGTTCCTCGA GAGGGTAGGAACACCGCT CGGTTTTCTATAATATTCA GAGGATCCCCAGCTGCGC	
MES157	GCGCACATGAGAATTCCAG CGACG	Forward primer for amplification of *D. hafniense ilvE* single-round transcription termination assay templates
MES158	GCGCAGCTGGGGATCCTCT G	Reverse primer for amplification of the *D. hafniense ilvE* WT and M9 single-round transcription termination assay templates
MES200	CCGAGCGGTGTTCCTACCC TC	Reverse primer for amplification of the M10 *D. hafniense ilvE* single-round transcription termination assay template
MES204	GCGCAGCTGGGGATCCTCT GAATATTATAAAAAACCG AGCGGTGTTCCTACCC	Reverse primer for amplification of the M11 *D. hafniense ilvE* single-round transcription termination assay template